Role of eddies in the interannual variability of Hadley cell strength

Rodrigo Caballero

Meteorology and Climate Centre, School of Mathematical Sciences, University College Dublin, Ireland

There is evidence from simplified atmosphere models that extratropical eddies strongly affect the Hadley cell mass flux. Here, we use reanalysis data to assess the role of eddy momentum transport in the interannual variability of northern hemisphere winter Hadley cell strength. We define a Hadley cell strength index and decompose it into an ENSO-related term and an uncorrelated remainder. Regressing these two time series onto the momentum budget shows that ENSO-related variability involves changes in momentum transport by tropical stationary waves, while non-ENSO variability is related to changes in the extratropical wave flux impinging on the tropics, with stationary waves dominant in the northern (winter) cell and transients dominant in the southern (summer) cell. Non-ENSO variability accounts for a large fraction of the interannual variance in Hadley cell strength, supporting the hypothesis that extratropical eddy stresses drive much of the zonally symmetric variability in the tropics.

1. Introduction

By affecting winds, clouds, humidity, precipitation and energy transport in the tropics, the Hadley cell plays a key role in the climate system. It is therefore important to understand the mechanisms underpinning its variability. Previous work [*Oort and Yienger*, 1996; *Quan et al.*, 2004] has shown significant co-variability between Hadley cell mass flux and the El Niño/Southern Oscillation (ENSO). Both these papers used composite analysis to show that the warm phase of ENSO is associated with a stronger and more equatorially symmetric Hadley circulation. On the other hand, recent work using simplified atmosphere models has shown that the propagation of midlatitude eddies into the tropics can also strongly affect Hadley cell strength [*Becker et al.*, 1997; *Kim and Lee*, 2001; *Walker and Schneider*, 2006], suggesting that much of the variability in the Hadley cell could be a response to changes in eddy forcing from the midlatitudes. Here, we explore this hypothesis through an observational assessment of the role played by eddy momentum transport in the interannual variability of Hadley cell strength.

Momentum transport is connected to the Hadley cell mass flux through the upper-tropospheric zonal momentum budget, which to leading order is a balance between zonal acceleration by meridional advection of absolute vorticity, and deceleration by eddy stresses:

$$(f+\overline{\zeta})\overline{v} = (1-Ro)f\overline{v} \approx S, \tag{1}$$

where overbars represent a zonal climatological mean and primes a deviation from the zonal mean, $\overline{\zeta} = -(a\cos\varphi)^{-1}\partial(\cos\varphi\,\overline{u})/\partial\varphi$ is the relative vorticity, $Ro = -\overline{\zeta}/f$ is a meridionally varying Rossby number [*Walker and Schneider*, 2006], and

$$S = \frac{1}{a\cos^2\varphi}\frac{\partial}{\partial\varphi}(\cos^2\varphi\,\overline{u'v'}) \tag{2}$$

is the horizontal eddy momentum flux divergence; other notation is standard.

If S is small, then angular momentum is conserved, $Ro \approx 1$ and the system is close to the nearly-inviscid axisymmetric regime in which the mass flux is determined purely by the diabatic forcing [*Held and Hou*, 1980]. If eddy momentum transport is very strong, on the other hand, then the subtropical jet is weak, Ro is small and the Hadley cell mass flux (proportional to the mass-weighted vertical integral of the meridional velocity v) is determined solely by the eddy stress, $v \approx S/f$. The observed value of Ro (Fig. 1a) peaks at about 0.5 for the northern hemisphere winter cell, suggesting that this cell is in an intermediate regime between the eddy-driven and axisymmetric limits. The summer cell, with $Ro \approx 0.2$, is closer to the eddy-driven limit. There are thus grounds for expecting an important influence of eddy stress on the variability of both cells.

Interannual variability in Hadley cell strength turns out to be relatively small compared to the mean (Sec. 3.1), so it is reasonable to linearize the momentum budget (1). With some rearrangement, we obtain

$$\delta v \approx \frac{\overline{v}}{1-Ro}\delta Ro + \frac{1}{(1-Ro)f}\delta S, \tag{3}$$

where δ indicates an interannual fluctuation around the climatological mean. Thus, increased mass flux can be balanced by increased Ro, or by increased eddy stress. Below, we will study the interannual variability of the momentum budget by regressing indices of Hadley cell strength onto the terms in (3). This analysis will show that changes in eddy stress do indeed play a crucial role in the momentum adjustment.

2. Data and climatology

We have analyzed both the ECMWF 40-year reanalysis (ERA40) [*Uppala et al.*, 2005] and the NCEP/NCAR 50-year reanalysis (NCEP) [*Kalnay et al.*, 1996], though for reasons of space we will mostly present ERA40 results here. The NCEP results are very similar and lead to the same qualitative conclusions. We use 6-hourly data on mandatory pressure levels to compute eddy fluxes. We focus on boreal winter, defined as December 1 to February 28 (DJF), which is when ENSO is most active.

To facilitate the discussion of interannual variability below, it is useful to first examine some aspects of the climatology. The DJF climatological mass streamfunction, Fig. 1a, has a well-known structure dominated by the northern cell, with ascent between 10°S and 10°N and descent between 10°N and 30°N. Fig. 1b shows that the upper-level momentum balance is well captured by (1). It also shows the partitioning of the eddy stress into stationary and transient

0094-8276/07/$5.00

components (stationary waves are defined here as those surviving seasonal averaging; transients are deviations from the seasonal mean). The two are of comparable magnitude within the tropics, though the stationary eddy stress is somewhat larger. Inspection of the Eliassen-Palm (EP) flux (Fig. 1c,d; this is the quasi-geostrophic flux defined as in [*Edmon et al.*, 1980]) shows that the transient eddy stress is due almost entirely to waves propagating equatorward from the midlatitudes, while the stationary eddy stress also has a significant contribution from tropical waves propagating poleward. As shown by *Dima et al.* [2005], these stationary tropical waves are the seasonal-mean Rossby wave response to zonally confined convective heating, especially over the western Pacific warm pool.

3. Interannual variability

3.1. Indices of Hadley cell strength

Following *Oort and Yienger* [1996], we compute the seasonal-mean mass streamfunction for each year in the dataset, and define a northern hemisphere Hadley cell strength index ψ^N as the maximum value of the streamfunction between 0° and 30°N. A well-known multi-decadal trend in ψ^N is present both in ERA40 and NCEP [*Tanaka et al.*, 2004; *Quan et al.*, 2004; *Mitas and Clement*, 2005]. The origin of this trend remains obscure; it is not reproduced in models [*Mitas and Clement*, 2006] and is likely an artefact of the reanalysis [*Bengtsson et al.*, 2004; *Held and Soden*, 2006]. Here, we focus on interannual variability by removing a linear trend from the ψ^N time series. The standard deviation of detrended ψ^N is about 1.7×10^{10} kg s^{-1}, or about 7% of the climatological mean, making the linearization in (3) plausible.

We now partition the detrended ψ^N into two components,

$$\psi^N = \psi^N_e + \psi^N_r, \tag{4}$$

where ψ^N_e is a linear regression onto the El Niño 3.4 index [*Trenberth*, 1997], while ψ^N_r is an uncorrelated remainder. In ERA40, the El Niño 3.4 index explains 24% of the detrended ψ^N variance, with a correlation coefficient of 0.49. The corresponding numbers for NCEP over its entire range (1949–2006) are 12% and 0.35, increasing to 16% and 0.41 when computed over the year range spanned by ERA40 (1959–2001). In all cases the correlations are significant at the 99% level using a 2-tailed t test, assuming successive years are uncorrelated. The considerable discrepancy between the two reanalyses highlights the difficulty of accurately capturing the divergent circulation, which is not well constrained by observations and is therefore sensitive to biases in the assimilating models [*Sardeshmukh and Hoskins*, 1987; *Andersson et al.*, 2005]. However, as previously noted, the qualitative nature of the regression results presented below is very similar in ERA40 and NCEP, so we believe it to be robust and not an artefact of the reanalysis procedure.

3.2. ENSO variability

Regressing ψ^N_e onto the mass streamfunction, Fig. 2e, reveals a pair of enhanced thermally direct cells straddling the equator in correspondence with warm ENSO events, accompanied by stronger subtropical jets (Fig. 2f); both features agree with previous work [*Oort and Yienger*, 1996; *Seager et al.*, 2003]. There is also an indirect cell centered around 20°N; the overall effect is one of narrowing and strengthening of the climatological cell (Fig. 1a). Enhanced poleward flow aloft (Fig. 2a) is balanced in the northern hemisphere by increased *Ro* (Fig. 2b) due to the stronger jet. The stationary eddy stress shows a significant weakening (Fig. 2d). As is clear from Fig. 2h, this is mostly due to decreased southward momentum flux by stationary tropical eddies, though there is also some reduction in the northward flux due to midlatitude eddies. Presumably, the stationary Rossby wave over the western Pacific warm pool weakens as convection moves to the central Pacific during El Niño events. The combination of stronger poleward vorticity advection and weaker eddy stress accounts for the enhanced subtropical jets seen in Fig. 2f. The transient eddies (Fig. 2c) play a secondary role, with some evidence of enhanced wave propagation into the deep tropics compensating in part for the weaker stationary eddy flux.

In the southern hemisphere, between the 0° and 10°S, the adjustment is quite different. Here, the response of upper-level v to ENSO is negative, and is balanced mostly by the eddy stresses, with stationary and transient waves giving roughly equal contributions. Since $\overline{v}$ is northward between the equator and about 13°S, the *Ro* term gives a positive contribution which partly offsets the eddy stress term. To summarize, in the northern hemisphere the adjustment is dominated by the *Ro* term and partially counteracted by the eddy stress term; in contrast, the southern hemisphere adjustment is dominated by the eddy stresses and partially counteracted by the *Ro* term.

3.3. Non-ENSO variability

Regressing ψ^N_r onto the mass streamfunction, Fig. 3e, reveals a remarkably simple pattern: a single direct cell in the northern hemisphere, of width comparable to the climatological cell's (Fig. 1a) but of lesser vertical extent. Meridional flow is strongly enhanced over a broad region in the upper troposphere (Fig. 3a). This increase is balanced almost entirely by increased stationary eddy stress (Fig. 3d). In contrast to what we saw above for ENSO-related variability, the change in stationary eddy stress is now due entirely to enhanced poleward momentum flux by midlatitude eddies (Fig. 3h). The increased eddy stress is accompanied by slightly weaker zonal flow throughout the tropics (Fig. 3f), and this leads to a small reduction in the *Ro* term poleward of 5°N (Fig. 3b). The overall change in zonal flow is small because the stronger eddy drag is counteracted by vorticity advection by the stronger Hadley cell. The transient eddies play a very minor role in the adjustment (Fig. 3c), though there is again evidence that they tend to counteract the effect of the stationary eddies.

4. Discussion and conclusions

We have defined two indices of Hadley cell strength, one proportional to the El Niño 3.4 index and the other orthogonal to it. Regressing these indices onto the linearized upper-tropospheric momentum budget (3) reveals very different patterns of adjustment to fluctuations in cell strength. For ENSO-related variability, increased cell strength is balanced in the northern hemisphere by increased *Ro*, while eddy stress decreases; for non-ENSO variability, we find the opposite scenario: increased cell strength is balanced by greater eddy stress with slightly reduced *Ro*. In the ENSO case, changes in eddy stress are due mostly to tropical stationary wave activity, while in the non-ENSO case they are due entirely to the extratropical stationary wave flux impinging on the tropics. The only feature common to both cases is that transients play a very minor role. Recalling that non-ENSO variability makes up over 70% of the total variance (Sec. 3.1), we conclude that changes in extratropical eddy stresses play a central role in driving much of the interannual variability in Hadley cell strength.

The above conclusions refer strictly to the dominant, cross-equatorial winter cell. It is interesting to contrast them with the behaviour of the weaker summer cell. Defining a summer Hadley cell strength index ψ^S as the minimum value of the streamfunction between 15°S and 35°S and performing a regression analysis analogous to that in Sec. 3 shows that interannual variability of summer cell strength is due almost entirely to fluctuations in transient eddy stresses, with both stationary eddies stresses and the *Ro* term playing negligible roles. These results are consistent with the small climatological value of *Ro* in the summer cell (Fig. 1a) and the weak stationary wave activity in the southern hemisphere.

In this brief paper, we have not examined the mechanisms behind the changes in extratropical eddy flux. There is evidence that stationary waves play a major role in the dynamics of the northern hemisphere winter annular mode (NAM) [*DeWeaver and Nigam*, 2000; *Limpasuvam and Hartmann*, 2000], and these fluctuations may cause greater planetary wave activity to be ducted into the tropics [*Chen et al.*, 2003, compare their Fig. 4a with our Fig. 3h]. However, the NAM index, a standard measure of annular mode activity [*Thompson and Wallace*, 2000, data obtained from www.cpc.noaa.gov], explains only 14% of the ψ_r^N variance in ERA40 and 8% in NCEP (if the total streamfunction index ψ^N is considered instead, the variance explained by the NAM index is reduced by half, to 7% in ERA40 and 4% in NCEP). Other work has pointed to the role of eddy transport of heat, rather than momentum, in driving changes in the Hadley cell [*Trenberth and Stepaniak*, 2003]. The two views are not necessarily incompatible, since increased fluxes of heat and momentum may occur simultaneously (the upward-pointing EP vectors near 20°N in Fig. 3h do in fact indicate increased low-level poleward heat flux by stationary waves, though this is largely cancelled by the opposite-signed response of transient waves, Fig. 3g). Questions remain, however, as to which is the dominant mechanism and how the two interact. Further work is needed to elucidate these issues.

Acknowledgments. Comments by Matt Huber, Jonathan Mitchell and two anonymous reviewers helped improve this paper. NCEP Reanalysis data provided by the NOAA/OAR/ESRL PSD, Boulder, Colorado, USA, from their web site at www.cdc.noaa.gov.

References

Andersson, E., et al. (2005), Assimilation and modeling of the atmospheric hydrological cycle in the ECMWF forecasting system, *Bull. Amer. Meteor. Soc.*, *86*, 387–402.

Becker, E., G. Schmitz, and R. Geprägs (1997), The feedback of midlatitude waves onto the Hadley cell in a simple general circulation model, *Tellus Ser. A*, *49*, 182–199.

Bengtsson, L., K. I. Hodges, and S. Hagemann (2004), Sensitivity of large-scale atmospheric analyses to humidity observations and its impact on the global water cycle and tropical and extratropical weather systems in ERA40, *Tellus Ser. A*, *56*, 202–217.

Chen, W., M. Takahashi, and H.-F. Graf (2003), Interannual variations of stationary planetary wave activity in the northern winter troposphere and stratosphere and their relations to NAM and SST, *J. Geophys. Res.*, *108D*(2), 15, doi: 10.1029/2003JD003834.

DeWeaver, E., and S. Nigam (2000), Do stationary waves drive the zonal-mean jet anomalies in the northern winter?, *J. Climate*, *13*, 2160–2176.

Dima, I. M., J. M. Wallace, and I. Kraucunas (2005), Tropical zonal momentum balance in the NCEP reanalyses, *J. Atmos. Sci.*, *62*, 2499–2513.

Edmon, H. J., B. J. Hoskins, and M. E. McIntyre (1980), Eliassen-Palm cross sections for the troposphere, *J. Atmos. Sci.*, *37*, 2600–2616.

Held, I. M., and A. Y. Hou (1980), Nonlinear axially symmetric circulations in a nearly inviscid atmosphere, *J. Atmos. Sci.*, *37*, 515–533.

Held, I. M., and B. J. Soden (2006), Robust responses of the hydrological cycle to global warming, *J. Climate*, *19*, 5686–5699.

Kalnay, E., et al. (1996), The NCEP/NCAR 40-year reanalysis project, *Bull. Amer. Meteor. Soc.*, *77*, 437–472.

Kim, H.-K., and S. Lee (2001), Hadley cell dynamics in a primitive equation model. Part II: Nonaxisymmetric flow., *J. Atmos. Sci.*, *58*, 2859–2871.

Limpasuvam, V., and D. L. Hartmann (2000), Wave-maintained annular modes of climate variability, *J. Climate*, *13*, 4414–4429.

Mitas, C. M., and A. Clement (2005), Has the Hadley cell been strengthening in recent decades?, *Geophys. Res. Lett.*, *32*, 3809–3813, doi:10.1029/2004GL021765.

Mitas, C. M., and A. Clement (2006), Recent behavior of the Hadley cell and tropical thermodynamics in climate models and reanalyses, *Geophys. Res. Lett.*, *33*, 1810–1813, doi: 10.1029/2005GL024406.

Oort, A. H., and J. J. Yienger (1996), Observed interannual variability in the Hadley circulation and its connection to ENSO, *J. Climate*, *9*, 2751–2767.

Quan, X.-W., H. F. Diaz, and M. P. Hoerling (2004), Change of the tropical Hadley cell since 1950, in *The Hadley cell: Past, present and future*, edited by H. F. Diaz and R. S. Bradley, Springer, Berlin.

Sardeshmukh, P. D., and B. J. Hoskins (1987), On the derivation of the divergent flow from the rotational flow: The χ problem, *Quart. J. Roy. Meteor. Soc.*, *113*, 339–360.

Seager, R., N. Harnik, Y. Kushnir, W. Robinson, and J. Miller (2003), Mechanisms of hemispherically symmetric climate variability, *J. Climate*, *16*, 2960–2978.

Tanaka, H. L., N. Ishizaki, and A. Kitoh (2004), Trend and interannual variability of Walker, monsoon and Hadley circulations defined by velocity potential in the upper troposphere, *Tellus Ser. A*, *56*, 250–269, doi:10.1111/j.1600-0870.2004.00049.

Thompson, D. W. J., and J. M. Wallace (2000), Annular modes in the extratropical circulation. Part I: Month-to-month variability, *J. Climate*, *13*, 1000–1016.

Trenberth, K. E. (1997), The definition of El Niño, *Bull. Amer. Meteor. Soc.*, *78*, 2771–2777.

Trenberth, K. E., and D. P. Stepaniak (2003), Seamless poleward atmospheric energy transports and implications for the Hadley circulation, *J. Climate*, *16*, 3706–3722.

Uppala, S., et al. (2005), The ERA-40 re-analysis, *Quart. J. Roy. Meteor. Soc.*, *131*, 2961–3012.

Walker, C. C., and T. Schneider (2006), Eddy influences on Hadley circulations: Simulations with an idealized GCM, *J. Atmos. Sci.*, *63*, 3333–3350.

Rodrigo Caballero, Meteorology and Climate Centre, School of Mathematical Sciences, University College Dublin, Belfield, Dublin 4, Ireland. (rodrigo.caballero@ucd.ie)

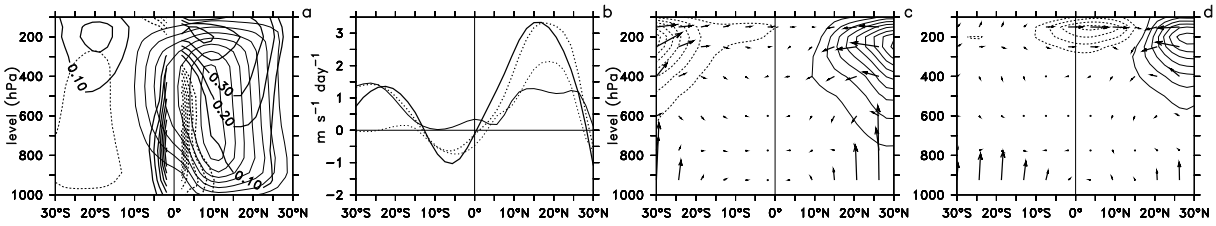

Figure 1. DJF climatology of the ERA40 reanalysis: (a) mass streamfunction (thin lines, c.i. 3×10^{10} kg s^{-1}, negative contours dashed, zero contour omitted) and Ro (thick lines, negarive contours dashed, c.i. 0.1); (b) momentum budget, Eq. (1), averaged between 300 and 100 hPa: $(1-Ro)f\overline{v}$ (thick solid), S (thick dotted), and partitioning of S into transient (thin solid) and stationary (thin dotted) contributions; (c) transient eddy momentum flux (c.i. 5 m^2 s^{-2}, negative contours dashed, zero contour omitted) and transient eddy EP flux (arrows); (d) as in (c) but for stationary eddies.

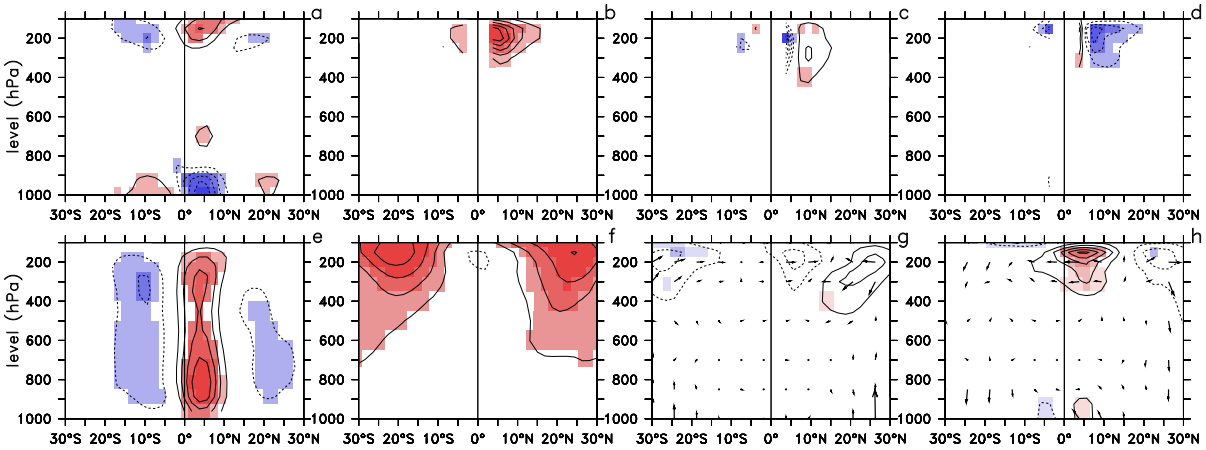

Figure 2. Top row: Regression of ENSO-related Hadley cell strength index ψ_e^N onto terms in the linearised momentum budget, Eq. (3): (a) δv; (b) δRo term; (c) transient eddy stress term; (d) stationary eddy stress term. Contour interval is 0.2 m s^{-1} throughout. Bottom row: Regression of ψ_e^N onto (e) mass streamfunction (c.i. 0.2×10^{10} kg s^{-1}); (f) zonal mean wind (c.i. 0.2 m s^{-1}); (g) transient eddy momentum flux (c.i. 0.3 m^2 s^{-2}) and EP flux (arrows); (h) as in (g) but for stationary eddies. In all panels, negative contours are dashed and the zero contour is omitted. Shading (with the same contour interval) is shown only where correlations are significant at the 99% level assuming no autocorrelation. The ψ_e^N time series used in all cases has been scaled so the the maximum value of the mass streamfunction in (e) is 1×10^{10} kg s^{-1}. In (b),(c) and (d) the near-equatorial region, where $1 - Ro$ is close to zero, has been blanked out.

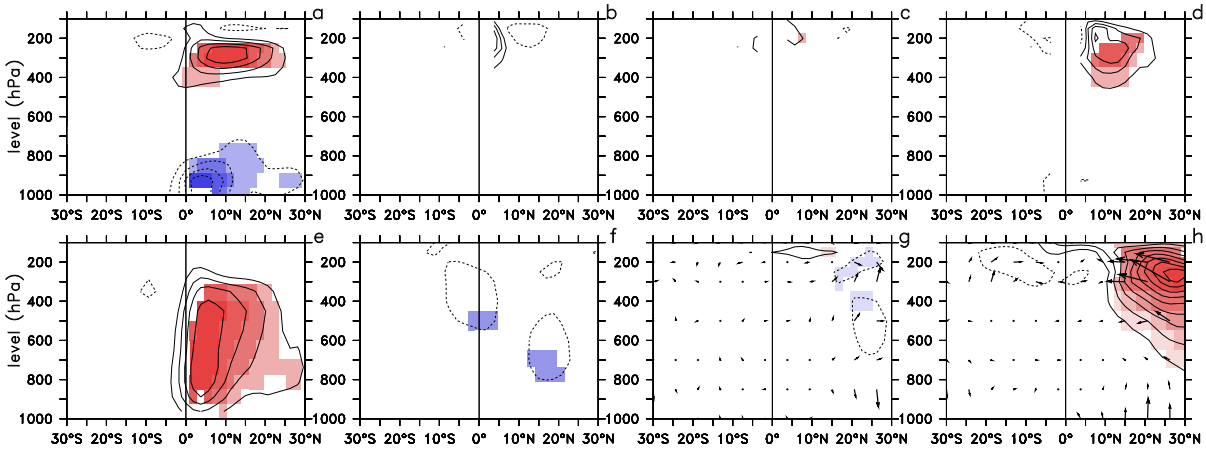

Figure 3. As for Fig. 2 but for non-ENSO index ψ_r^N.